Determining the Optimal Motorization for Low-Cost Tractor

Yassine Zahidi [1, 2], Mohamed El moufid [1, 2], Siham Benhadou [1, 2], Hicham Medromi [1, 2]

[1] EAS Research Team, Laboratory of Research in Engineering, ENSEM Casablanca, Morocco.
[2] Foundation of Research Development and Innovation in Sciences and Engineering (FRDISI).

E-mail: yassineezahidi@gmail.com, mohamedelmoufid@gmail.com,siham.benhadou@gmail.com, hmedromi@yahoo.fr

Abstract - The objective of present work is to evaluate three modes of motorization in order to determine the optimal one from an economic and ecological point of view. First, we define the tractive force Ft required to propel the tractor and attached implements. Then, we develop a model that allows us to calculate hourly consumption in diesel for 12 implements. Further, we propose a hybrid architecture with 25% electrification through an internal block diagram and calculate the cost of its hourly consumption and the quantity of CO2 when working with 12 implements. The results allow a comparative view of the three types of motorization. We find that the electric motorization will have a very high hourly consumption cost, with an almost unproductive quantity of CO2. On the other hand, the thermal engine can guarantee a low consumption cost, but with a significantly high quantity of CO2. Consequently, the hybrid engine offers the favourable conditions in terms of low consumption costs combined with a minimal amount of CO2.

Keywords - Tractor, hybrid architecture, Planetary gear unit, Engine, Implements.

I. INTRODUCTION

The need to feed more than 10 billion people on earth makes agriculture a very important industry [1]. Of all the machines, the tractor is the most widely used in the Sector [2].

The tractor is a wheeled or tracked vehicle used for the traction of agricultural machinery [3]. This explanation remains quite simple for a machine, which currently encompasses a multitude of applications. This machine has been considered as one of the advances, which have a great influence on the field of agriculture during the twentieth century [4].

The modern tractor is a very sophisticated beast that integrates the latest technologies in electronics, computers, data communication and satellite guidance systems [5].

The conventional agricultural tractors are equipped by internal combustion engines. As with other road transport modes, the pollution associated with the use of tractors is air pollution, linked to combustion gases containing polluting substances and released into the atmosphere. These emissions have bad impacts on several scales. Firstly, the high impact on the deterioration of air quality by (SO2, NOx, volatile organic co-components called VOCs, CO, particulates). Moreover, global warming by (CO2, CH4, N20, particles) [6]. In addition, the depletion of oil resources is becoming the main threat to human beings [7].

The EPA estimates that if left unchecked, off-road vehicles will contribute 33% of hydrocarbon (HC) emissions, 9% of carbon monoxide (CO), 9% of nitrogen oxides (NOx) and 2% of particulate matter (PM) emissions in the United States [8].

After the climate conferences (COP21, COP22) which are essentially focused on reducing greenhouse gases contributing to global warming, the majority of manufacturers are moving into the hybrid car with the symbol of a future clean environment as their main objective. an apparent lack of hybrid and fully electric technology in the agricultural machinery sector is still remaining [9].

II. STATE OF THE ART

A great deal of research has been carried out, leading to the replacement of internal combustion engine vehicles. Among the options currently being evaluated to replace internal combustion engine vehicles are Battery Electric Vehicles (BEV), Hybrid Electric Vehicles (HEV), Plug-in Hybrid Electric Vehicles (PHEV), Hydrogen Fuel Cell Electric Vehicles (HFCEV), etc.

Bradley and Frank's research on PHEVs shows significant benefits in terms of pollution, energy efficiency and sustainability of the transport and energy sector, by reducing oil consumption compared to internal combustion engine vehicles [10].

Lipman and Delucchi analyzed the manufacturing costs, retail prices and life-cycle costs of five gasoline-electric hybrid vehicles. They concluded that the inclusion of external social costs reduces the break-even cost of gasoline for HEVs by about $0.20 per gallon in the most likely case [11].

Mohamad abadi et al. evaluated economic, environmental, and social factors in selecting the best fuel-efficient vehicles for road transportation. They found that in the baseline scenario, where the weight of economic

parameters is more important, the gasoline-powered vehicle ranked higher than other vehicles. In the baseline scenario, where environmental parameters are more important, the hybrid vehicle was ranked first [12].

Delucchi and Lipman found that for EVs to be competitive with ICEVs, batteries must have lower manufacturing costs and a longer service life. They stated that it is more important to reduce the manufacturing cost of batteries to $100/kWh or less, and to increase the life cycle to 1200 or more per calendar life to 12 years or more and to target a specific energy of about 100 Wh/kg [13].

The Hybrid is in general a technology that combines a combustion engine with another electric motor to drive a vehicle [14] [15].

The principle of this engine is to operate these two engines in turn or simultaneously according to driving needs. The overall objective of this architecture is to combine the advantages of the two modes of motorization [16].

There are several types of hybridization, which can be mainly distinguished by the function of importance of their electrical system [17]:

- Start & Stop
- Mild-hybrid
- Full-hybrid
- Plug-in-hybrid

Understanding the disadvantages of conventional tractors was a challenge for us to think about hybrid tractors. In order to overcome the disadvantages.

In this work, we start by evaluating the energy requirement of our agricultural tractor. Secondly, we develop a power model based on thermal and electrical energy. Finally, we determine the operation of the various components of the hybrid tractor.

The table 1 in Appendix-I lists the main notations needed for the description of the model.

III. EVALUATING THE ENERGY REQUIREMENT

The tractive force required to propel the tractor and attached implements can be determined by equation 1 [18]:

$$F_t = F_{roll} + F_{air} + F_{acc} + F_{hill} + F_{imp} \quad (1)$$

A. The Needed Force for Implements

F_{imp} is a force parallel to the direction of travel (due to soil or crop treatment) required to propel the implements. The traction force required to pull many shallow seeding tools is mainly a function of the width of the tool and the travel speed. For tillage implements used at greater depths, the force depends on the soil texture, depth and geometry of the implements. There are mainly 2 types of implements. Some implements require drawbar power and others require PTO power. The force and power required for each kind of implement can be determined in different ways according to ASABE D497.4 [19].

For the implements requiring drawbar the needed force is calculated by equation 2 below:

$$F_{imp} = F_{i_s}[a + b(V) + c(V)^2]WT \quad (2)$$

Table II shows for every implement requiring a drawbar the selected parameters needed to calculate the necessary force using the above cited equation [19].

Relating to the implements requiring PTO power the needed power is presented in the table III below [19].

B. Rolling Resistance Force

Due to the deformation of the ground and the tire, rolling resistance is the friction of the tire on the road and the friction in the bearings. On soft surfaces, rolling resistance is mainly due to the deformation of the soil surface. It is proportional to the weight of the vehicle and can be determined using equation [20]:

$$F_{roll} = C_{roll} \cdot m \cdot g \quad (3)$$

C. Aerodynamic Drag

When a vehicle travelling at a given speed in an open area encounters an air force that resists its movement, this force is the aerodynamic drag, expressed by the following formula [21]:

$$F_{air} = \frac{1}{2} \rho_a A C_d (V + V_w)^2 \quad (4)$$

The density of air varies with temperature, altitude, and humidity. Larminie and Lowry stated that 1.25 kg m - 3 is a reasonable value to be used in most cases [21].

TABLE II. DRAFT PARAMETERS FOR IMPLEMENTS REQUIRING DRAWBAR

Name of Implement, Travel Speed											
Field Cultivator Primary Tillage, 11 km/h						**Moldboard Plow, 7 km/h**					
											
Machine Parameters			**Ground Parameters**			**Machine Parameters**			**Ground Parameters**		
a	**b**	**a**	**b**	**a**	**b**	**a**	**b**	**c**	**F1**	**F2**	**F3**
46	**2.8**	**0**	**1**	**0.85**	**0.65**	**652**	**0**	**0**	**1**	**0.7**	**0.45**
Rotary Hoe, 19 km/h						**Roller Harrow, 11 km/h**					
											
Machine Parameters			**Ground Parameters**			**Machine Parameters**			**Ground Parameters**		
a	**b**	**c**	**F1**	**F2**	**F3**	**a**	**b**	**c**	**F1**	**F2**	**F3**
600	**0**	**0**	**1**	**1**	**1**	**2600**	**0**	**0**	**1**	**1**	**1**

TABLE III. DRAFT PARAMETERS FOR IMPLEMENTS PTO POWER

Bette Harvest  **Travel Speed: 8 km/h. Power Requirement: 4.2 KWm^{-1}**	**Straw Tub grinder**  **Travel Speed: 0. Power Requirement: 8.4 KWh/t**
Flail Mower  **Travel Speed: 11 km/h. Power Requirement: 10 KWm^{-1}**	**Direct-cut Forage harvester**  **Travel Speed: 5-15 km/h. Power Requirement: 5.7 KWh/t**
Side Delivery Rake  **Travel Speed: 10 km/h. Power Requirement: 0.4 KWm^{-1}**	**Small Grains Combine**  **Travel Speed: 3-6.5 km/h. Power Requirement: 3.6 KWh/t**
Boom-Type Sprayer 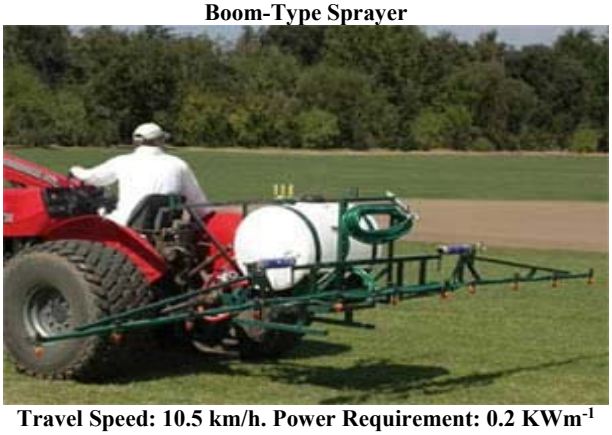 **Travel Speed: 10.5 km/h. Power Requirement: 0.2 KWm^{-1}**	**Grinder Mixer**  **Travel Speed: - km/h. Power Requirement: 4 KWh/t**

D. Hill Climbing Force

The climb force is the downward component of the weight when a vehicle climbs or descends a slope. Shukla and al. reported that slope climbing power describes the rate of change in potential energy associated with climbing [22].

However, Khanipour et al. mentioned that in the vehicle study the performance analysis only the uphill operation is taken into account, which can be expressed as [23]:

$$F_{hill} = m.g.\sin\alpha \quad (5)$$

E. Acceleration force

The acceleration force mainly represents the force providing the linear acceleration of the vehicle. Larminie and Lowry (2003) suggested that for accurate modelling of this parameter, it is necessary to consider the force required to rotate rotating parts faster. In other words, the rotational acceleration must be taken into account as well as the linear acceleration. Therefore, the acceleration force as a combination of linear acceleration and rotational acceleration could be expressed as [21]:

$$F_{acc} = F_{lacc} + F_{racc} \quad (6)$$

The linear acceleration is derived from newton's second law:

$$F_{lacc} = m \cdot a_{lacc} \quad (7)$$

The main portion of rotational acceleration is allocated to the electric motors due to their high angular speeds. The tire angular speed is calculated as:

$$\text{Tire angularspeed (rad s}^{-1}) = \frac{V}{r} \quad (8)$$

Therefore, the motor angular speed (Θ) and acceleration ($\ddot{\Theta}$) are given by equations and:

$$\theta = G\frac{V}{r} \quad (9)$$

$$\ddot{\theta} = G\frac{a_{lacc}}{r} \quad (10)$$

Similar to Newton's second law, the torque for angular acceleration is:

$$T_m = I.G.\frac{a_{lacc}}{r} \quad (11)$$

Quite often, Moment of inertia of the rotor of motor (I) is not known. Larminie and Lowry recommended that in such cases a reasonable approximation is formed by increasing the mass by 5% in equation 7 and ignoring the rotational acceleration term. However, in this case, rotational acceleration was computed using the method presented by Dhameja. In this method, Moment of inertia of the rotor of motor (I) is determined using only 3% of the weight of the vehicle. Therefore, the force at the wheels needed to provide the rotational acceleration force was derived as [21] [24]:

$$F_{racc} = T_m.\frac{G}{r} = I.\frac{G^2}{r^2}.a_{lacc} \quad (12)$$

By substituting the equation of the tractive force with the value of the different forces that compose it, we obtain the following equation:

$$F_t = C_{roll} \cdot m \cdot g + \frac{1}{2}\rho A C_d (V + V_w)^2 + m \cdot a_{lacc} + I.\frac{G^2}{r^2}.a_{lacc} + m.g.\sin\alpha + F_{imp} \quad (13)$$

IV. POWER MODEL BASED ON THERMAL OR ELECTRIC ENERGY CONSUMPTION

A. Thermal Energy Model

The diagram (figure 1) is a presentation of the variation in the pressure exerted on the piston as a function of its displacement (volume variations). The (ABCDEFGH) is the diagram of the theoretical cycle with mixed heat input of a supercharged four-stroke constant pressure diesel engine [8] [9] [10] [11].

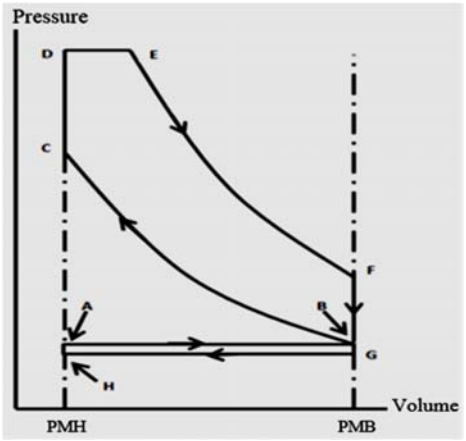

Fig. 1 Theoretical cycle represented on a diagram (P - V).

A1. The Indicated Work

The indicated work W_i of the real cycle is the sum of the work during all phases of the cycle:

$$W_i = \psi\left(W_{\text{Boucle supérieure}} + W_{\text{Boucle inférieur}}\right) = \psi W_{th} \quad (14)$$

Let ψ be the rounding coefficient of the thermodynamic diagram. Experimentally, it is between 0.95 and 0.97.

$$W_i = \psi(W_{AB} + W_{BC} + W_{CD} + W_{DE} + W_{EF} + W_{FB} + W_{BG} + W_{GH} + W_{HA}) \quad (15)$$

The exchanged work between the cylinder gazes and the piston is defined by:

$W_i = -\int PdV$. Which explains why the work of an isochoric transformation (at constant volume) is void.

Therefore: $W_{CD} = W_{FB} = W_{BG} = W_{HA}$.

The work of the piston in the intake phase is calculated by:

$W_{AB} = -\int_B^A PdV$. This transfer is at constant pressure $(P = P_A = P_B)$.

$$W_{AB} = -\int_A^B P_B dV = -P_B \int_A^B dV = -P_B(V_B - V_A) = -P_B V_B\left(1 - \frac{V_A}{V_B}\right) \quad (16)$$

Replacing the volume ratio with its expression according to $\varepsilon = \frac{V_B}{V_A}$:

$$W_{AB} = -(\varepsilon - 1)P_A V_A = -P_B V_B\left(1 - \frac{1}{\varepsilon}\right) \quad (17)$$

The Work during the exhaustion is calculated by: $W_{GH} = -\int_G^H PdV$.

This transfer is at constant pressure $(P = P_H = P_G)$.

$$W_{GH} = -\int_G^H P_G dV = -P_G \int_G^H dV = -P_G V_G\left(\frac{V_H}{V_G} - 1\right) = -P_H V_H\left(1 - \frac{V_G}{V_H}\right) \quad (18)$$

With: $\chi = \frac{P_A}{P_H} = \frac{P_B}{P_G}$ ($\frac{1}{\chi}$ is the pressure drop rate) and $\varepsilon = \frac{V_B}{V_A} = \frac{V_G}{V_H}$.

$$W_{GH} = -\frac{1}{\chi}(1 - \varepsilon)P_A V_A = -\frac{1}{\chi}\left(\frac{1}{\varepsilon} - 1\right)P_B V_B \quad (19)$$

The work of the lower loop of the theoretical cycle is the sum of two works of the transfers (intake and exhaust).

$$W_{(ABGH)} = W_{AB} + W_{GH} = -P_B V_B\left[\left(1 - \frac{1}{\varepsilon}\right) - \frac{1}{\chi}\left(\frac{1}{\varepsilon} - 1\right)\right] = \left(\frac{\varepsilon - 1}{\varepsilon}\right)\left(\frac{1 - \chi}{\chi}\right)P_B V_B$$

$$W_{(ABGH)} = W_{AB} + W_{GH} = -P_B V_B\left[\left(1 - \frac{1}{\varepsilon}\right) - \frac{1}{\chi}\left(\frac{1}{\varepsilon} - 1\right)\right] = \left(\frac{\varepsilon - 1}{\varepsilon}\right)\left(\frac{1 - \chi}{\chi}\right)P_B V_B \quad (20)$$

The Laplace law applied on BC polytrophic compression allows to write:

$$P_B V_B^{k_c} = P_c V_c^{k_c}$$

Whence:

$$P_B V_B V_B^{k_c - 1} = P_C V_C V_C^{k_c - 1} \quad (21)$$

So let $\varepsilon = \frac{V_B}{V_A}$, the equation (21) gives:

$$P_B V_B = P_C V_C\left(\frac{V_C}{V_B}\right)^{k_c - 1} = P_C V_C\left(\frac{1}{\varepsilon}\right)^{k_c - 1} = P_C V_C \frac{1}{\varepsilon^{k_c - 1}} \quad (22)$$

By replacing the value of $P_B V_B$ in the equation of $W_{(GHAB)}$, the work of the lower loop of the theoretical cycle becomes:

$$W_{(ABGH)} = \left(\frac{\varepsilon - 1}{\varepsilon}\right)\left(\frac{1 - \chi}{\chi}\right)P_B V_B = \frac{1}{\varepsilon^{k_c - 1}}\left(\frac{\varepsilon - 1}{\varepsilon}\right)\left(\frac{1 - \chi}{\chi}\right)P_C V_C \quad (23)$$

Compression is a polytrophic transformation characterized by Laplace's law $PV^{k_c} = cte$ This law allows to write:

$PV^{k_c} = P_B V_B^{k_c} = P_C V_C^{k_c}$, and then:

$$P = \frac{P_C V_C^{k_c}}{V^{k_c}} \quad (24)$$

The Work during compression is calculated by : $W_{BC} = -\int_B^C PdV$, By replacing the pressure value already calculated in the work formula:

$$W_{BC} = -\int_B^C \frac{P_C V_C^{k_c}}{V^{k_c}} dV \quad (25)$$

$$= -P_C V_C^{k_c} \int_B^C \frac{dV}{V^{k_c}} = \frac{-P_C V_C^{k_c}}{-k_c + 1}\left(V_C^{k_c} - V_B^{1 - k_c}\right)$$

$$W_{BC} = \frac{P_C V_C}{k_c - 1}\left(1 - \left(\frac{V_B}{V_C}\right)^{1 - k_c}\right) = \frac{P_C V_C}{k_c - 1}\left(1 - \frac{1}{\varepsilon^{k_c - 1}}\right) \quad (26)$$

The compression work can also be expressed:

$$W_{BC} = \frac{P_C V_C}{k_c - 1}\left(1 - \frac{V_B^{1 - k_c}}{V_C^{1 - k_c}}\right) = \frac{1}{k_c - 1}\left(P_C V_C - \frac{P_C V_C^{k_c}}{V_B^{k_c - 1}}\right) = \frac{1}{k_c - 1}\left(P_C V_C - \frac{P_B V_B^{k_c}}{V_B^{k_c - 1}}\right)$$

$$W_{BC} = \frac{P_C V_C}{k_c - 1}\left(1 - \frac{V_B^{1 - k_c}}{V_C^{1 - k_c}}\right) = \frac{1}{k_c - 1}\left(P_C V_C - \frac{P_C V_C^{k_c}}{V_B^{k_c - 1}}\right) = \frac{1}{k_c - 1}\left(P_C V_C - \frac{P_B V_B^{k_c}}{V_B^{k_c - 1}}\right) \quad (27)$$

Whence:

$$W_{BC} = \frac{1}{k_c - 1}(P_C V_C - P_B V_B) = \frac{1}{k_c - 1}\left(1 - \frac{1}{\varepsilon^{k_c - 1}}\right)P_C V_C \quad (28)$$

Work during isobaric combustion occurs at constant pressure $(P = P_D = P_E)$, which is calculated according to the following formula:

$$W_{DE} = -\int_D^E PdV = -P_E \int_D^E dV = -P_E(V_E - V_D) = -P_E V_D\left(\frac{V_E}{V_D} - 1\right) \quad (29)$$

with: $\lambda = \frac{P_E}{P_C}$ and $\rho = \frac{V_E}{V_D}$

whence:

$$W_{DE} = -\lambda(\rho - 1)P_C V_C \quad (30)$$

Work during polytrophic relaxation is derived from the following formula: $W_{BC} = -\int_E^F PdV$.

The polytrophic transformation is characterized by Laplace's law $V^{k_d} = cte$.

Then : $PV^{k_d} = P_E V_E^{k_d} = P_F V_F^{k_d}$

Whence : $P = \frac{P_E V_E^{k_d}}{V^{k_d}}$

$$W_{EF} = -\int_E^F \frac{P_E V_E^{k_d}}{V^{k_d}} dV = -P_E V_E^{k_d} \int_E^F \frac{dV}{V^{k_d}} = \frac{-P_E V_E^{k_d}}{(-k_d+1)\left(V_F^{1-k_d} - V_E^{1-k_d}\right)} \quad (31)$$

$$W_{EF} = \frac{P_E V_E^{k_d}}{k_d - 1}\left(\frac{V_F^{1-k_d}}{V_E^{1-k_d}} - 1\right) = \frac{P_E V_E}{k_d - 1}\left(\left(\frac{V_F}{V_E}\right)^{1-k_d} - 1\right) = \frac{P_E V_E}{k_d - 1}\left(\delta^{1-k_d} - 1\right)$$

$$W_{EF} = \frac{P_E V_E^{k_d}}{k_d - 1}\left(\frac{V_F^{1-k_d}}{V_E^{1-k_d}} - 1\right) = \frac{P_E V_E}{k_d - 1}\left(\left(\frac{V_F}{V_E}\right)^{1-k_d} - 1\right) = \frac{P_E V_E}{k_d - 1}\left(\delta^{1-k_d} - 1\right) \quad (32)$$

$$W_{EF} = \frac{P_E V_E}{k_d - 1}\left(\frac{1}{\delta^{1-k_d}} - 1\right) = \frac{-\lambda\rho}{k_d - 1}\left(\frac{1}{\delta^{1-k_d}} - 1\right) P_C V_C \quad (33)$$

With : $\lambda = \frac{P_E}{P_C}$, $\rho = \frac{V_E}{V_C}$ and $\delta = \frac{V_F}{V_E} = \frac{V_F}{V_C}\frac{V_C}{V_E} = \frac{\varepsilon}{\rho}$

$$W_{EF} = \frac{P_E V_E}{k_d - 1}\left(\frac{V_F^{1-k_d}}{V_E^{1-k_d}} - 1\right) = \frac{1}{k_d - 1}\left(\frac{P_E V_E^{k_d}}{V_F^{k_d-1}} - P_E V_E\right) = \frac{1}{k_d - 1}\left(\frac{P_F V_F^{k_d}}{V_F^{k_d-1}} - P_E V_E\right)$$

$$W_{EF} = \frac{P_E V_E}{k_d - 1}\left(\frac{V_F^{1-k_d}}{V_E^{1-k_d}} - 1\right) = \frac{1}{k_d - 1}\left(\frac{P_E V_E^{k_d}}{V_F^{k_d-1}} - P_E V_E\right) = \frac{1}{k_d - 1}\left(\frac{P_F V_F^{k_d}}{V_F^{k_d-1}} - P_E V_E\right) \quad (34)$$

then:

$$W_{EF} = \frac{1}{k_d - 1}\left(P_F V_F - P_E V_E\right) = \frac{-\lambda\rho}{k_d - 1}\left(\frac{1}{\delta^{1-k_d}} - 1\right) P_C V_C \quad (35)$$

The upper loop of the theoretical cycle is the sum of the work during compression and polytrophic relaxation, and isobaric combustion.

$$W_{(BCDEF)} = W_{BC} + W_{DE} + W_{EF} \quad (36)$$

$$W_{(BCDEF)} = \left(\frac{1}{k_c - 1}\left(\frac{1}{\varepsilon^{k_c-1}}\right) - \lambda(\rho - 1) - \frac{\lambda\rho}{k_d - 1}\left(1 - \frac{1}{\delta^{k_d-1}}\right)\right) P_C V_C \quad (37)$$

Calculation of the indicated work W_i is deduced by the following formula:

$$W_i = \psi W_{th} = \psi\left(W_{(ABGH)} + W_{(BCDEF)}\right) = \psi(W_{AB} + W_{BC} + W_{DE} + W_{EF} + W_{GH})W_i = \psi W_{th} = \psi\left(W_{(ABGH)} + W_{(BCDEF)}\right) = \psi(W_{AB} + W_{BC} + W_{DE} + W_{EF} + W_{GH}) \quad (38)$$

$$W_{th} = \left[\frac{(\varepsilon - 1)(1 - \chi)}{\chi\varepsilon^{k_c}} + \left(\frac{1}{k_c - 1}\left(1 - \frac{1}{\varepsilon^{k_c-1}}\right) - \lambda(\rho - 1) - \frac{\lambda\rho}{k_d - 1}\left(1 - \frac{1}{\delta^{k_d-1}}\right)\right)\right] P_C V_C$$

$$W_{th} = \left[\frac{(\varepsilon-1)(1-\chi)}{\chi\varepsilon^{k_c}} + \left(\frac{1}{k_c-1}\left(1 - \frac{1}{\varepsilon^{k_c-1}}\right) - \lambda(\rho-1) - \frac{\lambda\rho}{k_d-1}\left(1 - \frac{1}{\delta^{k_d-1}}\right)\right)\right] P_C V_C \quad (39)$$

$$W_i = \psi\left[\frac{(\varepsilon - 1)(1 - \chi)}{\chi\varepsilon^{k_c}} + \left(\frac{1}{k_c - 1}\left(1 - \frac{1}{\varepsilon^{k_c-1}}\right) - \lambda(\rho - 1) - \frac{\lambda\rho}{k_d - 1}\left(1 - \frac{1}{\delta^{k_d-1}}\right)\right)\right] P_C V_C$$

$$W_i = \psi\left[\frac{(\varepsilon-1)(1-\chi)}{\chi\varepsilon^{k_c}} + \left(\frac{1}{k_c-1}\left(1 - \frac{1}{\varepsilon^{k_c-1}}\right) - \lambda(\rho-1) - \frac{\lambda\rho}{k_d-1}\left(1 - \frac{1}{\delta^{k_d-1}}\right)\right)\right] P_C V_C \quad (40)$$

A.2. The Indicated Average Pressure

The indicated average pressure P_{mi} is the ratio of the indicated work and the engine displacement, expressed by the following relationship:

$$P_{mi} = \frac{-W_i}{C_y} \quad (41)$$

$$\frac{\psi\left[\frac{(\varepsilon-1)(1-\chi)}{\chi\varepsilon^{k_c}} + \left(\frac{1}{k_c-1}\left(\frac{1}{\varepsilon^{k_c-1}} - 1\right) + \lambda(\rho-1) + \frac{\lambda\rho}{k_d-1}\left(1 - \frac{1}{\delta^{k_d-1}}\right)\right)\right] P_C V_C}{C_y} \quad (42)$$

The volumetric compression ratio is defined by : $\varepsilon = \frac{C_y+V_m}{V_m}$

The dead volume as a function of displacement is :

$V_m = V_C = \frac{C_y}{\varepsilon-1}$

The application of the law of the place on polytrophic compression $P_C V_C^{k_c} = P_B V_B^{k_c}$. By the latter, the pressure at the end of compression P_C can be evaluated as a function of the pressure at the end of admission P_B :

$$P_C = P_{Cp} = P_B \left(\frac{V_B}{V_C}\right)^{k_c} = P_B \varepsilon^{k_c} = P_a \varepsilon^{k_c} \quad (43)$$

By replacing the values of P_C and V_C in the equation of the indicated mean pressure, we obtain :

$$P_{mi} = \frac{\psi \varepsilon^{k_c}\left[\frac{(\varepsilon-1)(1-\chi)}{\chi \varepsilon^{k_c}} + \left(\frac{1}{k_c-1}\left(1-\frac{1}{\varepsilon^{k_c-1}}\right) - \lambda(\rho-1) - \frac{\lambda\rho}{k_d-1}\left(1-\frac{1}{\delta^{k_d-1}}\right)\right)\right] P_a}{(\varepsilon-1)} \quad (44)$$

A3. The Indicated Power

Calculation of the indicated power P_i is the work performed during one second, calculated by the following formula:

$$P_i = W_i N_{c_y} n_{c_y} \quad (45)$$

With W_i : is the indicated work defined by:

$$|W_i| = P_{mi} C_y \quad (46)$$

Then the indicated power becomes:

$$P_i = \frac{n_{c_y} N C_y P_{mi}}{120} \quad (47)$$

Calculation of the indicated motor torque C_i (in N. m) could be calculated from the indicated power defined by:

$$P_i = \omega T_i \quad (48)$$

with:

$$\omega = \frac{2\pi N}{60} = \frac{\pi N}{30} \quad (49)$$

Whence:

$$T_i = \frac{P_i}{\omega} = \frac{30 P_i}{\pi N} \quad (50)$$

A4. The Indicated Efficiency

Calculation of the indicated efficiency and specific consumption: Calculation of the efficiency parameter indiqué η_i is the ratio of the heat transformed into indicated work W_i to the total amount of heat Q_{cb} received as a result of combustion:

$$\eta_i = \frac{W_i}{Q_{cb}} = \frac{W_i}{Q_{cb(isochore)}+Q_{cb(isobare)}} = \frac{W_i}{Q_{CD}+Q_{DE}} \quad (51)$$

A5. Indicated Specific Consumption

Calculation of the indicated specific consumption g_i indicated $\left(\frac{g}{kWh}\right)$ is the amount of fuel required to spend to obtain an indicated power of one kW for one hour. By representing the hourly consumption per C_h in $\left(\frac{kg}{h}\right)$, we obtain the specific consumption indicated as follows:

$$g_i = \frac{C_h 10^3}{P_i} \quad (52)$$

With : P_i in kW.

Relationship between effeciency and specific indicated consumption: The amount of heat supplied during one hour of combustion Q_h can be expressed by the following formula:

$$Q_h = C_h P_{CI} \quad (53)$$

By replacing the value of C_h from equation (52) in the formula of Q_h (53), we obtain:

$$Q_h = g_i P_i P_{CI} 10^{-3} \quad (54)$$

The indicated work performed for one hour in (kWh) :

$$W_{ih} = 3600 P_i \quad (55)$$

The replacement of W_{ih} and Q_h by their values in the formula of η_i gives:

$$\eta_i = \frac{W_{ih}}{Q_{CD}+Q_{DE}} = \frac{W_{ih}}{Q_h} \quad (56)$$

The case where P_{CI} is expressed in $\frac{kJ}{kg}$,the indicated efficiency is expressed by:

$$\eta_i = \frac{3600.10^3}{P_{CI} g_i} \quad (57)$$

From the indicated yield formula, the indicated specific consumption can be obtained g_i $\left(\frac{g}{kWh}\right)$:

$$g_i = \frac{3600.10^3}{\eta_i P_{CI}} \quad (58)$$

The Relationship between efficiency and average pressure indicated for a mass of one kg of fuel, the amount of heat released by its combustion in (kJ) :

$$Q = Q_{CD} + Q_{DE} = m_c P_{CI} = P_{CI} \quad (59)$$

A6. Torque

Torque relationship as a function of intake pressure:

$$T_i = \frac{P_i}{\omega} = \frac{30 P_i}{\pi N} \quad (60)$$

The replacement of P_i and P_{mi} by their values in the formula of C_i gives :

$$T_i = \frac{n_{cy} N C_y P_{mi}}{4\pi N} \tag{61}$$

$$\frac{n_{cy} N C_y \psi \varepsilon^{k_c}\left[\frac{(\varepsilon-1)(1-\chi)}{\chi\varepsilon^{k_c}}+\left(\frac{1}{k_c-1}\left(1-\frac{1}{\varepsilon^{k_c-1}}\right)-\lambda(\rho-1)-\frac{\lambda\rho}{k_d-1}\left(1-\frac{1}{\delta^{k_d-1}}\right)\right)\right]P_a}{4\pi N(\varepsilon-1)} \tag{62}$$

A7. The Power According to Hourly Consumption

The specific consumption indicated g_i as a function of intake pressure:

$$g_i = \frac{C_h 10^3}{P_i} \tag{63}$$

$$P_i = \frac{n_{cy} N C_y P_{mi}}{120} \tag{64}$$

The replacement of P_i and P_{mi} by their values in the formula of g_i gives :

$$g_i = \frac{C_h 10^3\, 120}{n_{cy} N C_y P_{mi}} \tag{65}$$

$$\frac{120 C_h 10^3(\varepsilon-1)}{n_{cy} N C_y \psi \varepsilon^{k_c}\left[\frac{(\varepsilon-1)(1-\chi)}{\chi\varepsilon^{k_c}}+\left(\frac{1}{k_c-1}\left(1-\frac{1}{\varepsilon^{k_c-1}}\right)-\lambda(\rho-1)-\frac{\lambda\rho}{k_d-1}\left(1-\frac{1}{\delta^{k_d-1}}\right)\right)\right]P_a} \tag{66}$$

from the equation (62) and (66) we obtain :

$$\frac{C_h 10^3\, 120(\varepsilon-1)}{n_{c_y} N C_y \psi \varepsilon^{k_c}\left[\frac{(\varepsilon-1)(1-\chi)}{\chi\varepsilon^{k_c}}+\left(\frac{1}{k_c-1}\left(1-\frac{1}{\varepsilon^{k_c-1}}\right)-\lambda(\rho-1)-\frac{\lambda\rho}{k_d-1}\left(1-\frac{1}{\delta^{k_d-1}}\right)\right)\right]g_i}$$

$$\frac{C_h 10^3\, 120(\varepsilon-1)}{n_{c_y} N C_y \psi \varepsilon^{k_c}\left[\frac{(\varepsilon-1)(1-\chi)}{\chi\varepsilon^{k_c}}+\left(\frac{1}{k_c-1}\left(1-\frac{1}{\varepsilon^{k_c-1}}\right)-\lambda(\rho-1)-\frac{\lambda\rho}{k_d-1}\left(1-\frac{1}{\delta^{k_d-1}}\right)\right)\right]g_i} \tag{67}$$

And :

$$T_i = \frac{C_h 120.10^3}{4 g_i \pi N} \tag{68}$$

from the equation (58) and (68) we obtain:

$$T_i = \frac{C_h 120 \eta_i P_{CI}}{3600\pi N} \tag{69}$$

Whence: $$P_i = \frac{C_h \eta_i P_{CI}}{3600} \tag{70}$$

B. Calculation of CO2 Emissions for Thermal Energy Model

The weight of a liter of diesel is 835grams.it contains 86.25% of carbon, which is 720 grams of carbon per liter. To burn this carbon into CO2, 1920 grams of O2 are needed. So, 720 grams of carbon plus 1920 grams of dioxide produces 2640 grams of CO2. Therefore, burning one liter of diesel fuel produces about 2.64 kg of carbon dioxide [12].

C. Electrical Energy Consumption Model

The Electrical energy consumption for electric vehicles is measured at the terminals of the battery, which supplies vehicles, in kWh. The consumption is the integration of the output power into the battery boundaries. The energy required for propulsion equals to the sum of resistance power, transmission losses and motor drive. With and are respectively the power losses due to the transmission and the engine drive [13].

$$P_{out} = \frac{V}{\eta_t \eta_m}\left(M_v g(f_r + i) + \frac{1}{2}\rho_a C_D A_f V^2 + M\delta\frac{dV}{dt}\right) \tag{71}$$

In electric vehicles, the recovery of braking energy, wasted in vehicles with internal combustion engines, can be recovered by operating a drive engine as a generator. The regenerative braking power at the battery terminals is expressed as follows [13]:

$$P_{in} = \frac{\alpha V}{\eta_t \eta_m}\left(M_v g(f_r + i) + \frac{1}{2}\rho_a C_D A_f V^2 + M\delta\frac{dV}{dt}\right) \tag{72}$$

Finally, the net energy consumption from the batteries is:

$$E_{out} = \int_{traction} P_{out} dt + \int_{braking} P_{in} dt. \tag{73}$$

V. A PROPOSED HYBRID MODEL FOR LOW-COST FARM TRACTOR

The hybrid vehicles are now classified into four main architectures: series hybrid, parallel hybrid, series-parallel hybrid, and complex hybrid [14].

The need to provide very high power requires the adoption of the full hybrid system with a complex architecture. The last-named one, as its name suggests, has a complex configuration, illustrated by the figure 2. This architecture seems to be similar to the parallel series hybrid, since the generator and electric motor are electric machines. However, the main differences are due to the bidirectional power flow of the electric motor in the complex hybrid and the unidirectional power flow of the generator in the series-parallel hybrid. This bidirectional power flow can allow versatile operating modes, in particular the three propulsion powers (thanks to the internal combustion engine and the first electric motor), which cannot be provided by the parallel series hybrid [32]. In addition, that the power converter is added to the motor/generator and motor. This makes complex hybrid full system more controllable and reliable than series-parallel full hybrid [33]. Hybrid vehicles combine more than one powertrain.

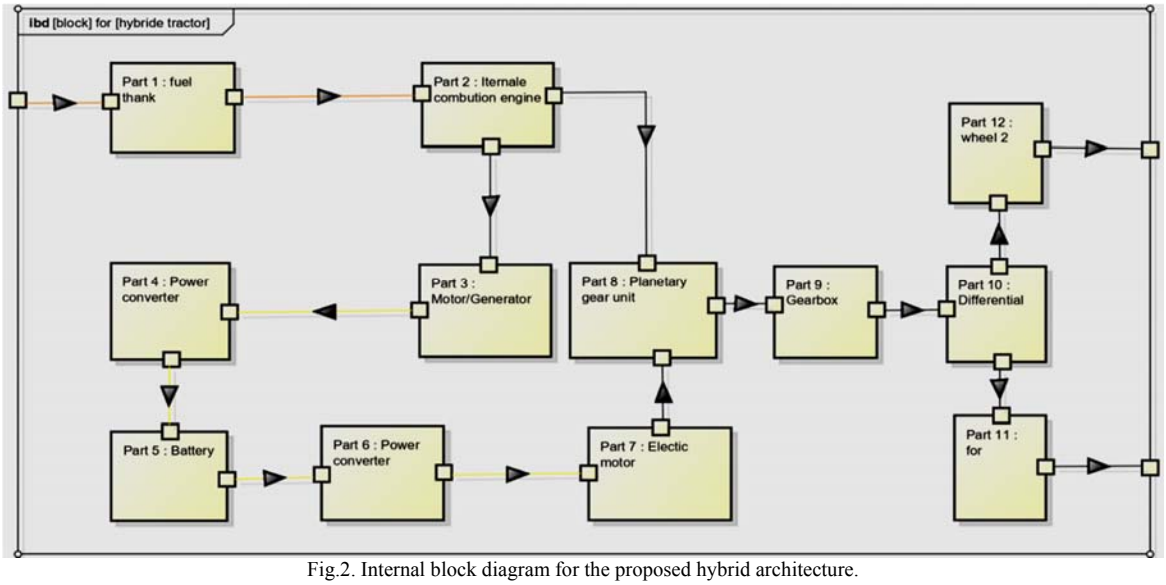

Fig.2. Internal block diagram for the proposed hybrid architecture.

This requires the use of à coupler to fully benefit from the efficiency. The characteristics of a speed coupling can be described by the following equation:

$$\omega_{out} = k_1\omega_{in1} + k_2\omega_{in2}$$

And

$$T_{out} = \frac{T_{in1}}{k_1} = \frac{T_{in2}}{k_2}$$

where k1 and k2 are constants associated with the actual design. Among the typical speed coupling devices is the planetary gear (Figure 3).

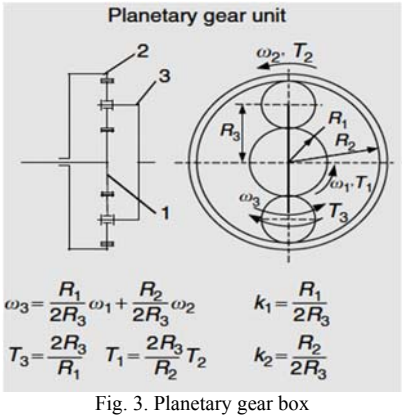

Fig. 3. Planetary gear box

The planetary gearbox (figure 3) consists of the sun wheel, the gear ring and the labelled cylinder head 1, 2 and 3, respectively. The relationship of angular velocity and torque between the three orifices indicates that the unit is a velocity coupling device, in which velocity, planetary and crown are added together and transmitted through the yoke. The constants k_1 et k_2 depend only on the radius of each wheel or the number of teeth of each wheel [13] [15].

VI. RESULTS AND DISCUSSIONS

This section is mainly structured around the table 4 below. The latter combines all the results obtained from the mathematical models and equations generated in this work.

The table is mainly composed of four main parts. The first is dedicated to the presentation of the powers necessary for the execution of agricultural operations by 12 tools, listed in the table. The implements are towed by a tractor with a weight of 2.5 t. As well as, the tools are classified into two categories, those that require a Drawbar power and those that require a PTO power.

The second major part of the table aims to highlight the consequences in terms of consumption costs and greenhouse gas emissions when using a tractor equipped with an internal combustion engine to carry out the tasks associated with the 12 tools already mentioned.

This large part, in turn, is divided into three sub-parts. The first is the numerical values of diesel consumption, calculated on the basis of the mathematical model already developed.

The second one contains the consumption values in cost terms, based on the values calculated in the first sub-section. And the third, lists the quantities of CO2 emitted in one working hour by each tool by the combustion engine.

From the results obtained in the first major part, we can see that the cost of diesel consumption is very reasonable for our case. But, there is a very high productivity of greenhouse gases (CO2).

Concerning the third major part of the table was devoted for pistachio nuts to the consequences in terms of consumption costs and greenhouse gas emissions, when using a tractor equipped with an electric motor to carry out the tasks associated with the listed tools. This large part

devoted to the electrical sector has its role and is broken down into three sub-sections.

The first is the numerical values of electricity consumption, calculated on the basis of the mathematical equations mentioned above. The second, expresses consumption in terms of cost. And the third, expresses the quantity of CO2 emitted in one hour and which equals 0 kg/h, as long as the electric motor does not produce CO2.

On the basis of the results of the second major party, we can see that this motorization does not have an impact on the environment, as long as it does not produce CO2, but to provide the power required, the cost will be very high.

The fourth and last major part of the table represents the determination of consumption costs and the amount of greenhouse gas emissions, if a hybrid engine is used, including 25% electrical intervention.

This large part, in turn, is divided into three sub-parts: The first sub-part is the numerical values of diesel consumption, calculated on the basis of the mathematical model already developed.

The second sub-part contains the consumption values in cost terms, based on the values calculated in the first sub-section. And the third sub-part, in which is listed the amount of CO2 emitted during one hour of work by each tool.

The results obtained show that with this hybrid engine, we can achieve the power required at a very reasonable cost and with less CO2 emissions.

Overall, the results obtained in the three main parts give a justification that with hybrid motorization we will have a combination of the advantages of both electrical and thermal architectures by minimizing consumption costs and CO2 emission rates.

TABLE VI. RESULTS

Name of Implement	Power Need		Diesel Fuel Internal Combustion Engine			Electrical Engine			Our Hybrid System		
			Fuel Consumption Kg/H	Consumption in Cost Terms (€)	CO_2 Emission (Kg/H)	Electrical Consumption kWh	Consumption in Cost Terms (€)	CO_2 Emission (Kg/H)	Fuel Consumption Kg/H	Consumption in Cost Terms (€)	CO_2 Emission (Kg/H)
Field Cultivator Primary Tillage	Soil Texture Fine	59.62 kW	12.16	14.60	38.44	214632	30048	0	9.12	10.95	28.83
	Soil Texture Medium	59.15 kW	12.07	14.48	38.16	212940	29811.6	0	9.05	10.86	28.62
	Soil Texture Coarse	58.80 kW	12	14.39	37.94	211680	29635.2	0	9	10.79	28.45
Moldboard Plow	Soil Texture Fine	36.93 kW	7.53	9.04	23.80	132948	18612.72	0	5.64	6.78	17.85
	Soil Texture Medium	36.55 kW	7.45	9.87	23.55	131580	18421.2	0	5.58	7.4	17.66
	Soil Texture Coarse	36.23 kW	7.39	7.79	23.36	130428	18259.92	0	5.54	5.84	17.52
Rotary Hoe	107.34 kW		21.90	26.28	69.24	386424	54099.36	0	16.42	19.71	51.93
Roller Harrow	65.23 kW		13.31	15.97	42.08	234828	32875.92	0	9.98	11.97	31.56
Bette Harvest	45.2 kWm^{-1}		9.22	11.06	29.15	162720	22780.8	0	6.91	8.29	21.86
Flail Mower	67.28 kWm^{-1}		13.73	16.47	43.40	242208	33909.12	0	10.29	12.35	32.55
Side Delivery Rake	52.1 kWm^{-1}		10.63	12.75	33.60	187560	26258.4	0	7.97	9.56	25.2
Boom-Type Sprayer	54.6 kWm^{-1}		11.14	13.37	35.22	196560	27518.4	0	8.35	10.02	26.41
Straw Tub Grinder	8.4 KWh/t		1.71	2.05	5.40	8.4	1.167	0	1.28	1.53	4.05
Direct-Cut Forage Harvester	206240 KWh/t		11.71	10.61	37.02	206213.7	28869.918	0	8.78	7.95	27.76
Small Grains Combine	118897.5 KWh/t		7.46	8.96	23.58	18300.76	2562.10	0	5.59	6.72	17.68
Grinder Mixer	4.0 KWh/t		0.84	1	2.65	4	0.56	0	0.63	0.75	1.98

VII. CONCLUSION

Agriculture is one of the most important industry in the world and the tractor is mainly considered as the axial machine in this sector. In order to reduce greenhouse gases according to the recommendations of climate conferences (COP21, COP22). This work represents a comparative study between three types of engine (thermal, electric and hybrid) from both an economic and ecological point of view. In a first step, we develop the equation of the traction force required to propel the tractor and each attached tool. Thus we present an appropriate mathematical model, expressing power as a function of hourly diesel consumption. In addition, we propose a hybrid architecture for the low-cost tractor with 25% electrification.

The results calculated for each of the 12 selected implements based on the developed models are listed in a table, allowing a comparative visibility. The latter showed that the electric motor will have a very high hourly consumption cost, with almost zero CO2 emissions. Similarly, the internal combustion engine has a low consumption cost, but with a significantly high quantity of CO2. Hybrid engines have demonstrated a low consumption cost associated with a minimal quantity of CO2. Therefore, the engine provides the most favourable conditions for our case. Finally, the experimental study of the performance of the proposed architecture will be the subject of future studies. As well as a study of the possibility of integrating renewable energy into our architecture.

REFERENCES

[1] N. V. Fedorof, "Food in a future of 10 billion," no. 11 (2015), 2015.

[2] r. gifford, "Agricultural mechanisation in development. Guidelines for strategy formulation," FOOD AND AGRICULTURE ORGANIZATION OF THE UNITED NATIONS, rome, 1981.

[3] O. J. Bawden, "DESIGN OF A LIGHTWEIGHT, MODULAR ROBOTIC VEHICLE FOR THE SUSTAINABLE INTENSIFICATION OF BROADACRE AGRICULTURE," School of Electrical Engineering and Computer Science, 2015.

[4] DK, The Tractor Book: The Definitive Visual History, 2015.

[5] G. G. W. Manuel Götz, "Electrification and Driver Assist Technology in the ZF Innovation Tractor," ATZoffhighway worldwide, pp. 16-21, 2016.

[6] S. L. S. B. e. É. D.-F. Frédéric Vigier, "COMMENT DÉTERMINER LA CONSOMMATION DES AUTOMOTEURS," Sciences Eaux & Territoires, pp. 46-53 , 2012.

[7] K. S. Deffeyes, "Beyond oil: the view from Hubbert's Peak," Hill and Wang, new york, 2006.

[8] u. s. E. p. Agency, "Non-road engines and airpollution,Office of Mobile Sources,EPA 420-F-94-003," Washington, 1996.

[9] L. B. Ben McFADZEAN, "AN INVESTIGATION INTO THE FEASIBILITY OF HYBRID AND ALL-ELECTRIC AGRICULTURAL MACHINES," Series A. Agronomy,, vol. LX, no. 2285-5807, pp. 500-511, 2017.

[10] F. A. D. Bradley TH, "demonstrations and sustainability impact assesment for plug-in hybride electric vehicles," Renew Sust Energy Rev, vol. 13, no. 115-28, 2009.

[11] D. M. Lipman TE, "A retail and lifecycle cost analysis of hybrid electric vehicles," Transport Res D, vol. 11, no. 115-32, 2006.

[12] T. G. K. A. Mohamadabadi HS, "Development of a multi-criteria assessment model for ranking of renewable andnon-renewable transportation," Energy, vol. 34, no. 112-25, 2009.

[13] L. T. Delucchi MA, "An analysis of the retail and lifecycle cost of battery-powered electric vehicles.," Transport Res D, vol. 6, no. 371-404, 2001.

[14] B. Destraz, "Assistance énergétique à base de super condensateurs pour véhicules à propulsion électrique," l'Université de Lausanne, lausane, 2008.

[15] S. Kermani, "Gestion énergétique des véhicules hybrides : de la simulation à la commande temps réel," l'Université de Valenciennes et du Hainaut , Valenciennes, 2009.

[16] B. GINDROZ, "Optimization of a Predictive Drive Strategy for a Plug-In Hybrid," the Royal Institute of Technology, KTH Department of Vehicle Engineering, Stockholm, Sweden, 2014.

[17] E. L. Oriol Saperas, "OEM's Electric Vehicle Strategies: Risk Assessment," World Electric Vehicle Journal, vol. 5, no. 2032-6653, pp. 911-952, 2012.

[18] A. K. A. J. H. M. K. A. A. S. H. Mousazadeh, "Optimal Power and Energy Modeling and Range Evaluation of a Solar Assist Plug-in Hybrid Electric Tractor (SAPHT)," American Society of Agricultural and Biological Engineers, vol. 53, no. 2151-0032, pp. 1025-1035, 2010.

[19] C. A. S. o. A. Engineers, "ASAE D497.4 MAR99 Agricultural Machinery Management Data," American Society of Agricultural Engineers, USA, 2000.

[20] B. P. J. C. a. D. R. Szadkowski, "A Study of Energy Requirements for Electric and Hybrid Vehicles in Cities," in CESURA, Poland, 2003.

[21] J. L. James Larminie, Electric Vehicle Technology Explained, J. Wiley, 2003.

[22] N. R. A. a. B. C. M. A. K. Shukla, "FUTURE CARS: THE ELECTRIC OPTION," Curr. Sci, vol. 77, no. 9, p. 1141-1146, 1999.

[23] A. K. M. E. a. W. J. S. Khanipour, "Conventional Design and Simulation of an Urban Hybrid Bus," International Journal of Mechanical and Mechatronics Engineering, vol. 1, no. 4, pp. 146-152, 2007.

[24] S. Dhameja, "Testing and computer based modeling of electric vehicle batteries.," in Electric Vehicle Battery Systems, oxford,UK, Newnes Publishers, 2001, p. 161-190.

[25] G. M. A. MOURTADA, Transmission De La Chaleur, Beyrouth: l'Université Libanaise, Section des sciences de l'ingénieur, 1998.

[26] J. SISI, Principes De Thermodynamique, Bibliothèque Nationale du Québec, 1981.

[27] M. MORKOS, Moteurs À Combustion Interne, beyrout: Université Libanaise,, 2002.

[28] P. Arquès, Moteurs alternatifs à combustion interne, Ellipses, 1992.

[29] S. K. A. R. . P. Shalini, "Environment Sustainabilty within Supply Chain of Automobiles," Eurasian Journal of Analytical Chemistry, no. 13, pp. 211-216, 2018.

[30] Y. G. E. G. E. Mehrdad Ehsani, Modern electric, Hybride Electric,and Fuel Cell Vehicles, 2005: CRC PRESS.

[31] R. P. S. Karan C. Prajapati, "Hybrid Vehicle: A Study on Technology," International Journal of Engineering Research & Technology, pp. 1076-1082, 2014.

[32] C. C. Chan, "The State of the Art of Electric,Hybrid, and Fuel Cell Vehicles," Proceedings of the IEEE, pp. 704-718, 2007.

[33] C. W. T. Siang Fui Tie, "A review of energy sources and energy management system in electricvehicles," Renewable and Sustainable Energy Reviews, p. 82–102, 2013.

[34] M. T. S. B. Sif Eddine GuenidiM, "Model based Design of an Electrical Hybrid Vehicle with Energy Management," International Journal of Computer Applications, vol. 97, no. 17, pp. 35-41, 2014.

APPENDIX –I:
TABLE I. MAIN NOTATIONS USED

Symbol	Description
A	Point at the entry of the cylinder on the P-V diagram
a, b and c	Machine-specific parameters (dimensionless)
A_f	Vehicle Frontal Area (m^2)
B	Point at the end of amission on the P-V diagram
C	Point at the end of compression on the P-V diagram
C_h	Hourly Fuel Consumption (kg fuel/h)
C_y	Engine unit displacement (kcal/kg.K)
C_{roll}	Tire Rolling resistance Coefficient
C_D	The aerodynamic drag coefficient that characterizes the shape of the vehicle
D	Point at the end of isochronous combustion on the P-V diagram
$\frac{dV}{dt}$	Acceleration
E	Point at the end of isobaric combustion on the P-V diagram,
E_{out}	The net energy consumption from the batteries
F	Point at the end of the trigger on the P-V diagram
f_r	Rolling resistance coefficient.
F_{roll}	Rolling resistance force (N)
F_{air}	Aerodynamic drag (N)
F_{acc}	Force required for linear and angular acceleration (N)
F_{hill}	Hill climbing force (N)
F_{imp}	The needed force for implements (N)
F_{lacc}	Force is required for linear acceleration (N)
F_{racc}	Force is required for rotational acceleration (N)
F_t	Tractive force (N)
F_{i_s}	Soil texture adjustment parameter (dimensionless)
G	Gear ratio from electric motor to tire drive shaft.
g_i	Indicated specific consumption (g/kWh)
g	Gravity acceleration (m s^{-2})
I	Moment of inertia of the rotor of motor (kg m^2).
i	Road grade
i_s	1 for fine, 2 for medium, and 3 for coarse textured soils (dimensionless)
k_d	Polytropic expansion coefficient
k_c	Coefficient of polytropic compression
m	Combination of tractor and operator mass (kg)

Symbol	Description
M_v	The total mass of the vehicle
M	Modulation index, adjustable within the 0 to 1 range
n_{c_y}	The number of cylinders
N	The rotational speed of the crankshaft, in revolutions per minute (rpm)
N_{c_y}	The number of cycles per second for a four-stroke engine (for a two-stroke engine, $N_{c_y} = \frac{N}{60}$)
P_{CI}	Lower calorific value of fuel (42 MJ/kg of fuel)
P_i	Indicated power (kW)
P_{mi}	Average indicated pressure (Pa)
Q_A	Quantity of heat brought to the cycle (kcal),
r	Drive tire radius (m)
T_i	Indicated engine torque (N.m)
T	Tillage depth (cm) for major tools or 1 (dimensionless) for minor tillage tools and seeding implements.
T_m	Torque for angular acceleration (N m)
V	Field speed (km h^{-1})
V_m	Cylinder dead volume (m^3)
V_w	Wind velocity (km h^{-1})
W	Machine width (m or number of rows or tools)
W_i	The Indicated engine work (J)
W_{th}	The theoriqual work (J)
ω	The speed of rotation $\left(\frac{rad}{s}\right)$
χ	Pressure drop rate
δ	Relaxation rate
ε	Volumetric compression ratio
η_i	Indicated yield
λ	Rate of pressure rise
ρ	Preliminary relaxation rate
ψ	Diagram Rounding Coefficient
ρ_a	Air density (1.29 kg/m3)
α	is the slope of the road or field (rad).
α_b	$(0 < \alpha < 1)$ is the percentage of the total braking energy that can be applied by the electric motor, called the regenerative braking factor.
θ	Motor angular speed (rad s^{-1})
$\ddot{\theta}$	Motor angular acceleration (rad s^{-1})
δ	The mass factor